The Journal of Neuroscience, November 1, 2002, 22(21):9176–9184

Expression and Functional Characterization of GABA Transporters in Crayfish Neurosecretory Cells

Julieta Garduño, Sergio Elenes, Jorge Cebada, Elizabeth Becerra, and Ubaldo García

Department of Physiology, Biophysics, and Neuroscience, Centro de Investigación y de Estudios Avanzados, 07360 Mexico City, Mexico

The effect of GABA on membrane potential and ionic currents of X-organ neurons isolated from the crayfish eyestalk was investigated. Under voltage-clamp conditions, GABA elicited an inward Na^+ current followed by a sustained outward chloride current. Sodium current was partially blocked in a dose-dependent manner by antagonists of GABA plasma membrane transporters such as β-alanine, nipecotic acid, 1-[2([(diphenylmethylene)imino]oxy)ethyl]-1,2,5,6-tetrahydro-3-pyridinecarboxylic acid hydrochloride (NO 711), and SKF89976-A at concentrations between 1 and 100 μM. This current was totally blocked by the combined application of NO 711 (5 μM) and β-alanine (50 μM). We obtained an EC_{50} of 5 μM and a Hill coefficient of 0.97 for the GABA transport mediated response. These results together with studies of immunolocalization using antibodies against neuronal vertebrate GABA transporters (GATs) indicate the presence of GAT-1- and GAT-3-like proteins in X-organ neurons. To isolate the sustained outward Cl^- current, extracellular free sodium solution was used to minimize the contribution of GAT activity. We concluded that this current was caused by the activation of $GABA_A$-like receptors with an EC_{50} of 10 μM and a Hill number of 1.7.

To assign a functional role to the GATs in the X-organ sinus gland system, we determine the GABA concentration (0.46–0.15 μM) in hemolymph samples using HPLC.

In summary, our results suggest that a sodium-dependent electrogenic GABA uptake mechanism has a direct influence on the excitability of the X-organ neurons, maintaining an excitatory tone that is dependent on the circulating GABA level.

Key words: Procambarus clarkii; *crustaceans; crayfish; X-organ sinus gland system; peptidergic neurons; GABA transporters; $GABA_A$ receptors*

GABA is the major inhibitory neurotransmitter in both the CNS and PNS of vertebrates (Iversen and Kelly, 1975; Martin, 1976) and invertebrates (Iversen and Kravitz, 1968; Kerkut et al., 1969; Sattelle, 1990). After the neurotransmitter has been released, its postsynaptic action must be terminated by activation of a sodium-dependent high-affinity GABA uptake system, which is present in presynaptic terminals and glial cells (Atwood, 1976; Krnjevic, 1984; Erecinska, 1987; Kanner and Schuldiner, 1987; Dingledine et al., 1988). Thus, GABA transporters modify the neurotransmitter concentration in the synaptic cleft, producing a reduction in the availability of GABA acting on its receptors. Nevertheless, this is not the only postsynaptic effect, because GABA uptake is an electrogenic process that increases membrane conductance; therefore the transport activity might contribute directly to modify the excitability in postsynaptic neurons. It has been established that GABA transporters (GATs) belong to a sodium chloride-dependent transporter of 12 putative transmembrane helices. This family also includes transporters for serotonin, dopamine, norepinephrine, Gly, and Tau. Mammalian GABA transporters have been cloned and classified into four different members (GAT-1 to GAT-4) by differential amino acid sequences and pharmacological properties (Guastella et al., 1990; Borden et al., 1992; Clark et al., 1992; Liu et al., 1993; Yue et al., 1993; Swan et al., 1994). Two invertebrate GABA transporters that share certain similarities with the mammalian GATs have been cloned, expressed, and pharmacologically characterized. The first one was obtained from *Manduca sexta* embryos and designated MasGAT (Mbungu et al., 1995); it was functionally tested in *Xenopus* oocytes by measuring the [^{3}H]GABA transport. The other one, isolated from the cabbage lopper *Trichoplusia ni* and named TrnGAT (Gao et al., 1999), showed high identity with MasGAT as well as GAT-1; however, it was pharmacologically different from GAT-1 by the inability of cyclic GABA analogs, such as nipecotic acid, to inhibit [^{3}H]GABA uptake by TrnGAT.

In this work we have examined the effects of GABA on membrane potential as well as the associated ionic currents in secretory neurons from the crayfish X-organ, defined as neurons with axonal terminals that are specialized for the release of hormones to the circulatory system (Duan and Cooke, 2000). The X-organ sinus gland system is the major neurosecretory structure in crustaceans; it participates in the control of different functions such as molting, regulation of blood sugar levels, tegumentary and retinal pigment position, locomotion, and neuronal activity (García and Aréchiga, 1998). Both spontaneous electrical activity and hormone release in X-organ neurons are regulated by environmental and endogenous influences such as light, stress, and circadian rhythms that are mediated by synaptic and hormonal influences. Recently, it has been shown that GABA and glutamate activate different ionotropic receptors and chloride conductances in crab X-organ neurons (Duan and Cooke, 2000), whereas serotonin, acting on metabotropic receptors, activates calcium-dependent high-conductance potassium channels in a neuronal subpopula-

Received March 27, 2002; revised Aug. 15, 2002; accepted Aug. 15, 2002.

This work was supported by Grant 26400-N from Consejo Nacional de Ciencia y Tecnología, Mexico. We are grateful to Dr. Luisa Rocha and Leticia Neri Bazán from Centro de Investigación y de Estudios Avanzados (CINVESTAV) Pharmacobiology Department for technical HPLC assistance and to Dr. Agustín Guerrero from CINVESTAV Biochemistry Department for critical reading of this manuscript. We also thank Smithkline Beecham London for providing the SKF89976-A.

Correspondence should be addressed to Dr. Ubaldo García, Department of Physiology, Biophysics, and Neuroscience, Centro de Investigación y de Estudios Avanzados, Avenida Instituto Politécnico Nacional 2508, San Pedro Zacatenco, 07360 Mexico City, Mexico. E-mail: ugarcia@fisio.cinvestav.mx.

tion that produces red pigment-concentrating hormone (Alvarado-Alvarez et al., 2000).

In the present paper, we have determined that GABA produces a depolarization associated with neuronal firing, followed by a repolarization that suppresses electrical activity. The excitatory phase was caused by the activation of an electrogenic uptake system, whereas the inhibitory phase was associated with the activation of a ligand-gated chloride conductance. To suggest a physiological role for the transporter-mediated current, we determined the extracellular GABA concentration.

MATERIALS AND METHODS

Chromatography. Animals were anesthetized in ice and then 200 μl of hemolymph samples were obtained from the coxal membrane articulation of the legs. These samples were precipitated with 0.4 M perchloric acid (1:1, v/v), and the resulting mixture was vortex and filtered through Millipore membranes of 0.22 μm by centrifugation at 5000 rpm for 15 min. An aliquot of 10 μl from the supernatant of each sample was mixed with 10 μl of 0.1 M perchloric acid and derivatization reagent (6 μl), which was prepared as follows: 15 mg of *o*-phtaldialdehyde was dissolved in 300 μl of methanol and added with 2.8 ml of 0.4 M tetrapotassium borate buffer plus 25 μl of 2-β-mercaptoethanol.

Off-line derivatization procedure was performed, and the samples were vortexed briefly; after 120 sec, they were injected into the HPLC column. The HPLC system consisted of Millenium 32 from Waters with a fluorescence detector model 474 (Waters) operated at an excitation wavelength of 360 nm and an emission wavelength of 450 nm. Separations were achieved using a Novapack C_{18} conventional column (particle size 60 Å; 150 × 3.9 mm). Ternary gradient elution was used. Mobile phase A consisted of 40 mM sodium acetate buffer in 10% methanol, adjusted to pH 5.7, and mobile phase B consisted of 8 mM sodium acetate buffer in 80% methanol, adjusted to pH 6.7 with acetic acid. The mobile phases were degassed in an ultrasonic bath before they were used. The elution profile was as follows: 0 min 77% A, 23% B; 0.5 min 55% A, 45% B; 6.5 min 26% A, 74% B; 9.75 min 3% A, 97% B; 18.4 min 77% A, 23% B; the flow rate was 500 μl/min.

The calibration curves were adjusted from chromatograms of standard solutions that contained 0.1, 0.3, or 0.5 ng/μl of Asp, Glu, Gln, Gly, Tau, Ala, and GABA (Sigma, St. Louis, MO). The peak area ratios of the standards versus the GABA concentration were adjusted by least-squares linear regression analysis, using the system manager (Waters).

Dissection and culture. Adult crayfish *Procambarus clarkii* of either sex at the intermoult period were collected from Rio Conchos (Chihuahua, Mexico) and adapted to laboratory conditions for 2 weeks under a 12 hr light/dark cycle at room temperature (20–26°C). Eyestalks were excised and placed in chilled crayfish saline solution, consisting of (in mM): 205 NaCl, 5.4 KCl, 2.6 $MgCl_2$, 13.5 $CaCl_2$, and 10 HEPES adjusted to pH 7.4 with NaOH. The exoskeleton, muscles, and connective tissue surrounding the neural structures were carefully removed under a dissecting microscope. Isolated X-organs were incubated with 200 μg/ml collagenase dispase (Boehringer Mannheim, Indianapolis, IN) dissolved in modified Leibovitz L-15 (Invitrogen) culture medium for 60 min. The enzyme was washed out, and the X-organ neurons were dissociated by gentle suction through fire-polished micropipettes as described previously (García et al., 1990) and plated onto a 200 μl recording chamber that was precoated with Concanavalin A (type III; Sigma). The ionic composition of the culture medium was adjusted to that of the crayfish saline solution. An additional 5.5 mM glucose, 2 mM L-glutamine, 16 μg/ml gentamycin (Shering Plough), 5 μg/ml streptomycin (Sigma), and 5 U/ml penicillin (Sigma) were added. Culture cells were kept in darkness for 24 hr before the experiments were conducted.

Electrophysiology. Current- and voltage-clamp experiments in the standard whole-cell configuration or using the perforated-patch configuration (Marty and Neher, 1995) were performed in X-organ cells plated in the recording chamber mounted on the stage of an inverted microscope (Nikon, Diaphot). The cells were superfused continuously with crayfish saline solution, but in some experiments the bath solution was modified by reducing the sodium concentration to 102.5 mM or totally replaced by *N*-methyl-D-glucamine. Current- and voltage-clamp recordings were performed using an Axopatch 200A amplifier (Axon Instruments, Foster City, CA) and then low-pass filtered at 10 kHz with a four-pole Bessel filter and stored on computer disk using commercially available hardware and software (Axon Instruments). The capacitive current response to a −5 mV voltage step from −60 mV was recorded in all cells and periodically tested during the experiment. In the whole–cell experiments, the series resistance was estimated in the range of 2.5–4.5 MΩ and reduced by 50–70% using the compensation circuit of the amplifier. Recording electrodes (2–3 MΩ) from borosilicate glass (Sutter Instruments) were filled with a solution consisting of (in mM): 195 KCH_3SO_4, 12 KCl, 2 $CaCl_2$, 2 $MgCl_2$, 5 EGTA-Na, and 10 HEPES (whole-cell mode solution) or filled with 207 KCl, 2 $CaCl_2$, 2 $MgCl_2$, 5 EGTA-Na, and 10 HEPES plus 150 μg/ml gramicidin (perforated-patch mode solution).

Immunocytochemical staining. X-organ cells with 36 hr in culture were fixed in Stefanini's solution (2% paraformaldehyde, 15% picric acid, and 1% sucrose dissolved in 0.18 M PBS, adjusted at 7.4 pH) for 30–35 min. Then the cells were rinsed three times and permeabilized with PBS containing 0.01% saponin and 20% sucrose for 10 min. To prevent nonspecific binding, the cells were incubated for 30 min in a blocking solution consisting of 0.5% normal goat serum (Vector Laboratories, Burlingame, CA) in PBS. After washing, the cells were incubated overnight at 4°C in the following primary antibodies at 1:100 dilutions: GAT-1 (rabbit polyclonal antibody to aa 270–288 of the rat; Alpha Diagnostic International); GAT-3 (rabbit polyclonal antibody to the C-terminal region, aa 613–627; Alpha Diagnostic International), or $GABA_A$ (mice monoclonal antibody to α-chain $GABA_A$ receptor; Boehringer Mannheim). The cells were rinsed three times with PBS and incubated with a goat anti-rabbit biotinylated antibody (Vectastain, Vector Laboratories) at 5 μg/ml in PBS for 40–60 min. The cells were incubated with Vectastain ABC reagent (Vector Laboratories) for 30 min. Finally, the stain was developed with 0.01% 3,3′-diaminobenzidine in PBS plus 0.01% H_2O_2 for 3 min. All of these steps were followed for control cells except the incubation with the primary antibodies.

GABA, β-alanine, and nipecotic acid were purchased from Sigma; NO 711 hydrochloride and picrotoxin were from Research Biochemicals (Natick, MA); SKF89976-A was a gift from Smithkline Beecham. All solutions were prepared on the day of use.

RESULTS

GABA hemolymph content

Well defined chromatographic peaks for Asp, Glu, Gln, Gly, Tau, Ala, and GABA were obtained from standard solutions containing 0.1, 0.3, or 0.5 ng/μl from each amino acid. Their retention times were 3.2, 4.1, 4.9, 6.2, 6.9, 7.7, and 8.3 min, respectively (Fig. 1*A*). Peaks with identical retention times were identified in hemolymph samples. Figure 1*B* shows the chromatographic profile of a sample obtained at 6 P.M. that contained on average (n = 6 ± SD) the following concentrations (in μM): 1.6 ± 0.14 Asp, 3.8 ± 1.08 Glu, 3.6 ± 0.41 Gln, 3.3 ± 0.23 Gly, 1.7 ± 0.46 Tau, 2.9 ± 0.46 Ala, and 0.46 ± 0.11 GABA (Fig. 1*B*). These levels fluctuate during the day, but particularly the GABA levels decrease until 0.15 μM in samples obtained at midnight. To date there have been no published reports about the GABA hemolymph content or changes in its concentration during the day in crustaceans.

Effects of GABA in cultured X-organ cells

As illustrated in Figure 2, low GABA concentrations (0.1–0.5 μM) evoked a sustained depolarization that produced neuronal firing, whereas concentrations ranging between 1 and 10 μM evoked a complex response. This consisted of an early transient depolarizing phase associated with neuronal firing followed by a repolarization phase that suppress the electrical activity. During GABA washout, a later depolarizing phase was evident, suggesting that the ionic current responsible for the early transient depolarizing phase was still active.

The GABA depolarizing phase was not blocked by picrotoxin, a well characterized noncompetitive antagonist of $GABA_A$ receptors (Sattelle, 1990). The experiment illustrated in Figure 3 shows that 5 μM GABA induced only a sustained depolarization associated with neuronal firing when the GABA pulse was applied in the presence of picrotoxin. This result is similar to those

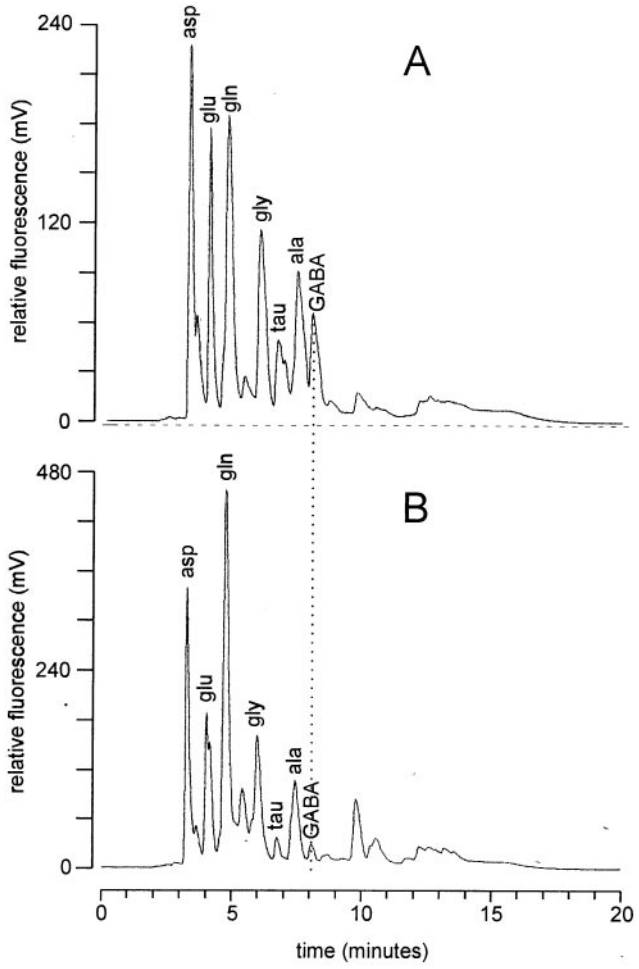

Figure 1. Presence of GABA in the crayfish hemolymph. *A*, Chromatogram of a standard solution of amino acids. *B*, Typical chromatogram from a hemolymph sample obtained at 6 P.M. The *dotted line* indicates that the retention time for GABA was the same for both samples (see details in Materials and Methods).

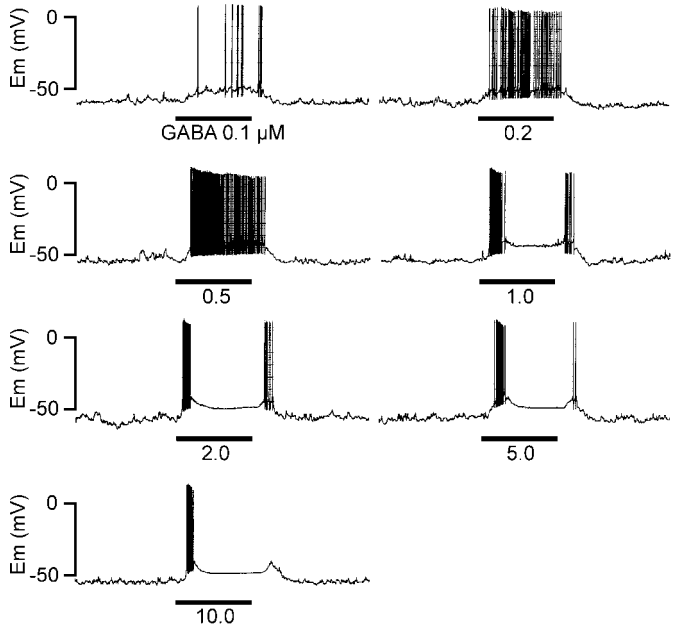

Figure 2. Effects of GABA concentration on membrane potential. All of the traces were obtained from the same X-organ neuron, in the gramicidin–perforated-patch configuration. The washout interval between each GABA application was 3 min, and the membrane potential was maintained at −60 mV. Note that GABA concentrations between 0.1 and 0.5 μM produced only depolarization associated with neuronal firing, whereas concentrations between 1 and 10 μM evoked a transient depolarization followed by a repolarization that suppressed the neuronal firing. In these traces, the presence of a final depolarization during the GABA washout was evident. The *solid bar* below the traces represents both the GABA applications and time scale (1 min). *Em*, Membrane potential.

observed with low GABA concentration (Fig. 2). To explore the ionic nature of the depolarizing responses, the extracellular sodium was substituted with *N*-methyl-glucamine. Under this condition and even in the presence of picrotoxin, GABA did not evoke any changes in membrane potential (Fig. 3), suggesting that the depolarizing phase was sodium dependent, whereas the repolarizing phase could be attributed to an increase in chloride permeability.

To explore the changes in membrane conductance evoked by GABA, recordings were performed in either current- or voltage-clamp conditions in the perforated-patch configuration. The early depolarizing phase of the GABA response was associated with a transient inward current, whereas the repolarizing phase was associated with a sustained outward current that drastically reduced the membrane resistance, which in turn induced suppression of the neuronal firing in current-clamp recordings. As shown in Figure 4, the current amplitude and its corresponding decay in membrane resistance were dependent on the GABA concentration; the average reductions of the input resistance during GABA superfusion were 27, 80, and 90% for concentrations of 1, 10, and 100 μM, respectively. These effects are representative of those observed in six other neurons.

We next examined the voltage dependence of the GABA-induced currents using the perforated-patch configuration by plotting peak currents against membrane potentials from −120 to 20 mV. Figure 5*A* shows that the inward current progressively decreased as the holding potential was changed to positive values; although this current did not reverse, it was reduced to undetectable levels. Figure 5*B* depicts pronounced inward rectification to an extent that was undetectable between 0 and 20 mV (Fig. 5*B*, ○). This rectification is characteristic of GAT-associated currents (Quick et al., 1997). In contrast, the sustained outward current increased at depolarizing values and reversed at −75 mV (Fig. 5*B*, ●). This value corresponded to the chloride equilibrium potential (E_{Cl^-}) estimated in our laboratory when we studied the chloride current generated by inhibitory glutamate receptors in crayfish X-organ neurons in culture. To confirm that the outward current is generated by chloride, in some experiments the cells were incubated with 5 μM picrotoxin during the GABA pulse applications (Fig. 5*C*, *middle traces*); such experimental conditions allowed us to isolate the inward current. These results suggest that chloride channels associated with GABA receptors mediate the sustained outward current, whereas the transient inward current could be caused by the activation of an electrogenic GABA uptake mechanism, similar to those described in the crayfish stretch receptor (Kaila et al., 1992) and the horizontal cells of the catfish retina (Cammack and Schwartz, 1993).

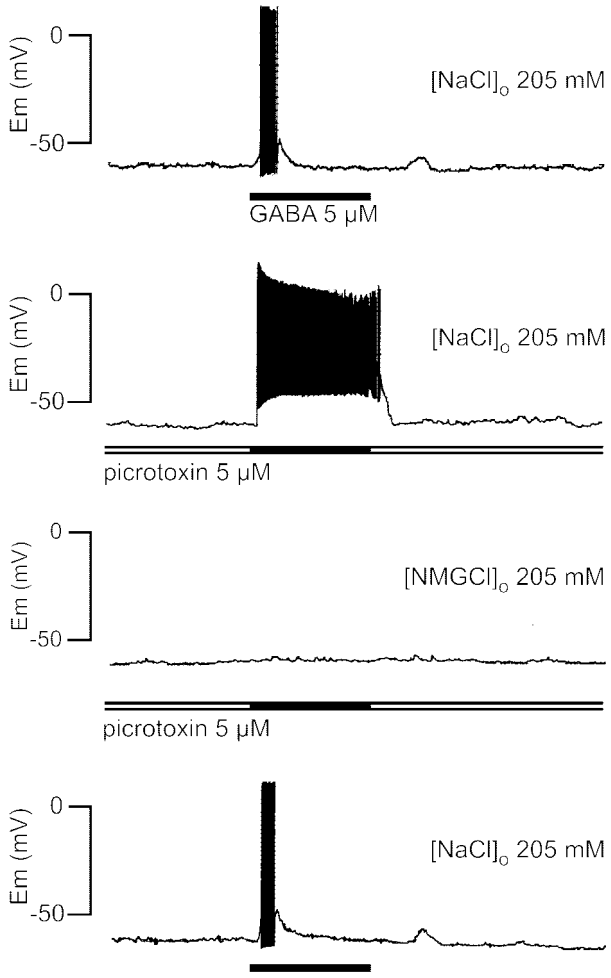

Figure 3. Role of sodium and effect of picrotoxin on the GABA-evoked response in X-organ neurons. The GABA response in crayfish saline solution was modified by picrotoxin, which suppressed the repolarizing phase, but it was completely abolished when the external solution was switched to one in which all sodium chloride had been replaced with *N*-methylglucamine chloride. After the return to crayfish saline solution (*bottom trace*), the response to GABA was restored. The traces were obtained in the gramicidin–perforated-patch configuration; the washout interval between each GABA application was 3 min, and the membrane potential was maintained at −60 mV. Similar results were obtained from seven additional cells. The *horizontal bars* represent 1 min.

Sodium dependence of the GABA-induced transient inward current

An important feature of GABA transport systems is their absolute dependence on extracellular sodium (Erecinska, 1987; Kanner and Schuldiner, 1987). To demonstrate the Na^+ dependence of the inward current, we explored the GABA response in different extracellular sodium concentrations. Neurons were superfused with crayfish saline, low-sodium or free-sodium solutions, and for each condition 10 μM GABA was tested on both voltage- and current-clamp modes. In the low-sodium solution, the amplitude of inward current decreased consistently by 45%, whereas the sustained outward current increased by 25%. Furthermore, in the free-sodium solution the inward current was not detectable, and the sustained outward current increased by 70% (Fig. 6*A*, *current traces*). It was evident that during GABA removal, the time course of the later depolarization was more prominent in the crayfish saline solution than those observed in low-sodium solution (Fig. 6*A*, *voltage traces*), suggesting that the later depolarization was Na^+ dependent. The effects of the sodium substitution on the amplitude of the GABA-induced currents are summarized in Figure 6*B*.

To isolate the Na^+-dependent current, cells in the conventional whole-cell configuration were voltage clamped at −62.6 mV to reduce the chloride current; this value corresponded to the E_{Cl^-} under our recording conditions. As shown in Figure 7*A*, the application of 1 μM GABA induced a sustained inward current; higher concentrations resulted in a sigmoidal concentration–response curve where 100 μM GABA elicited the maximal inward current. The experimental values were normalized and fitted to the Michaelis–Menten equation, indicating that 5 μM GABA induced the half-maximal response and 0.5 μM was the lowest concentration capable of generating the sodium inward current (Fig. 7*B*). The dose–response relationship was linearized, and a Hill coefficient of 0.95 was calculated by linear regression (Fig. 7*C*).

Isolation of the outward Cl^- current

To corroborate that the outward current was caused exclusively by an increase in chloride permeability, cells were superfused with sodium-free solution, and current traces were obtained in the standard whole-cell configuration. In addition, two internal solutions were used to establish an E_{Cl^-} of 0 mV (perforated patch) or −62.6 mV (standard whole cell). A voltage ramp was applied from −120 to 30 mV at 7.5 mV/sec from a holding membrane potential of −60 mV before and during GABA superfusion. In Figure 8*A*, *trace a* correspond to the steady-state current obtained before GABA superfusion when the E_{Cl^-} was 0 mV. The leak current at −60 mV was <20 pA, and near −30 mV a negative slope current was activated that reached its maximum value at −20 mV; this was followed by an outward current. *Traces b* and *c* correspond to the net GABA-induced current obtained at E_{Cl^-} of both 0 and −62.6 mV, respectively. We subtract the control traces from those obtained during GABA superfusion to minimize the influence of the noninduced GABA currents. Figure 8*B* summarizes the results obtained with 16 (■) and 10 (●) neurons recorded under the two different E_{Cl^-} values. The average values were fitted to a linear regression that crossed the voltage axis at −62.6 and −3 mV, respectively.

As illustrated in Figure 8*C* (concentration–response curve), the chloride current started at 2 μM GABA, the EC_{50} corresponded to 10 μM, and the saturating concentration was reached between 50 and 100 μM. The linearized concentration–response curve yielded a Hill coefficient of 1.7 (Fig. 8*D*). This value indicates that at least two GABA molecules are necessary to activate a single GABA receptor, in agreement with previous studies (Sakmann et al., 1983; Hattori et al., 1984; Bormann and Clapham, 1985; White, 1992).

Pharmacology of the GABA-induced transient inward current

Several compounds that block GABA plasma membrane transport in mammalian CNS were tested for their ability to antagonize the sodium inward current in X-organ neurons. The inhibitors of GAT-1, nipecotic acid, NO 711, and SKF89976-A as well as β-alanine, a potent and selective GAT-3 inhibitor, blocked the sodium inward current in a dose-dependent manner. However, none of them alone was able to block fully the sodium current. In fact, the superfusion of nipecotic acid (10 μM) induced a sustained inward current that reduced the amplitude of the GABA-induced inward current by 50% (Fig. 9*A*, *top traces*). As a consequence of

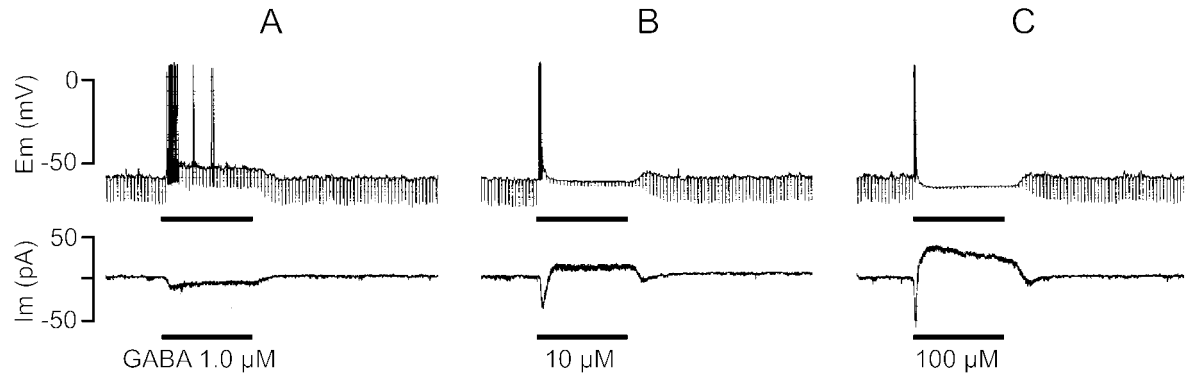

Figure 4. Changes in input resistance evoked by GABA and the relation between membrane potential and membrane currents. Pairs of recordings obtained in current clamp or voltage clamp with the gramicidin–perforated-patch configuration. The application of hyperpolarizing current pulses (10 pA, 500 msec, 0.4 Hz) allowed us to estimate the membrane resistance changes during GABA superfusion. Note that the increase in membrane conductance evoked by GABA was concentration dependent and its correlation with the time course and amplitude of the membrane currents. All of the traces were obtained at −60 mV from the same neuron. The *horizontal bars* represent 1 min.

this reduction, an increase in the amplitude of GABA-induced outward chloride current was observed. Note in the current-clamp traces that during the nipecotic acid superfusion, the resting membrane potential was depolarized and the repolarizing phase reached more negative potentials (Fig. 9*A*, *bottom traces*). This effect can be attributed to a competitive blockage excerpted on the GABA transporters.

The pharmacological results are summarized in Figure 9*B*. Note that the combination of NO 711 (5 μM) with β-alanine (50 μM) totally abolished the sodium inward current. These observations strongly suggest that X-organ neurons expressed GABA transporters that have a pharmacological profile similar to that described in mammalian CNS. To confirm these results, we performed immunocytochemical studies for plasma membrane transporters GAT-1 and GAT-3.

Immunocytochemistry

Additional evidence for the presence of GABA receptors and transporters in the crayfish X-organ neurons is depicted in Figure 10. The antibody directed to GAT-1 recognizes the sequence located between aa 270 and 288, whereas the antibody directed to GAT-3 recognizes the C-terminal region (aa 613–627). Finally, the antibody directed to the GABA receptor recognizes the α1 subunit. Nonspecific binding of antibodies was determined as indicated in Materials and Methods. From the observation of 640 cells, we concluded that all neurons in X-organ expressed $GABA_A$-like receptor as well as the GAT-1- and GAT-3-like transporters.

DISCUSSION

Various excitatory actions of GABA have been described in crustaceans. In the visual system of the crayfish, GABA induces a depolarization of tangential cells in the medulla externa of the optic peduncle while decreasing their membrane conductance (Pfeiffer-Linn and Glantz, 1989). In a selected population of neurosecretory cells in the X-organ of the crayfish isolated eyestalk, GABA elicits depolarizing responses and bursts of action potentials; these effects are blocked by picrotoxin but not by bicuculline, and they involve a reduction of the input resistance (García et al., 1994). Recently, in the stomatograstric ganglion neurons, lateral pyloric and piloric, of the crab *Cancer borealis*, it was shown that GABA and muscimol elicits a picrotoxin-sensitive depolarizing response, the ionic nature of which remains unre-

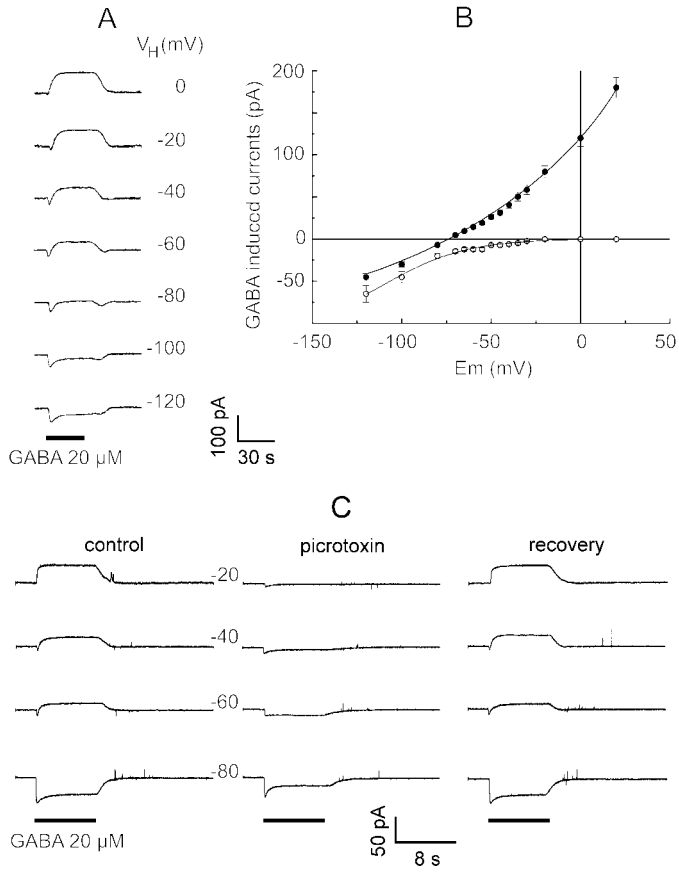

Figure 5. *A*, Effects of 20 μM GABA on membrane current at holding potentials from −120 to 20 mV. Recordings were obtained with the gramicidin–perforated-patch configuration. The cell was held at the new potential for at least 30 sec before the application of GABA, and the washout interval between each GABA pulse was 3 min. *B*, Peak currents evoked by GABA plotted against membrane potential. *Open* and *filled circles* correspond to the peak amplitude of the inward current and the sustained outward current, respectively. Each *point* corresponds to the mean values ± SEM for $n = 10$. *C*, Effect of picrotoxin (5 μM) on the GABA-evoked currents at the signaled holding potentials. The blockage of the chloride current allowed the isolation of the GABA-induced inward current.

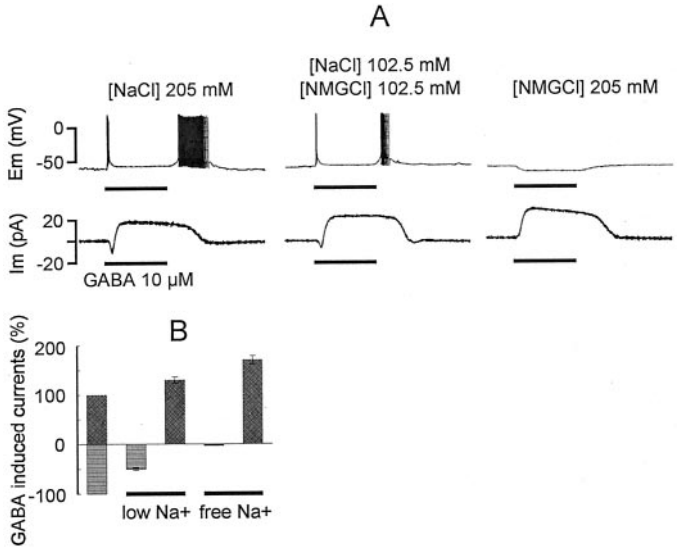

Figure 6. Sodium dependence of the inward current evoked by GABA. *A*, Recordings from the same neuron obtained at −60 mV in current or voltage clamp in the gramicidin–perforated-patch configuration, during the superfusion of 10 μM GABA dissolved in extracellular solutions with different sodium concentrations. Note that the inward current decreased in the low-sodium solution and was completely abolished in the free-sodium solution. *B*, Histogram of the mean effects of the extracellular sodium concentration on the amplitude of the outward and inward currents induced by GABA. Note that the outward current amplitude increased when the inward current diminished. *Columns* are normalized mean values ± SEM for $n = 16$.

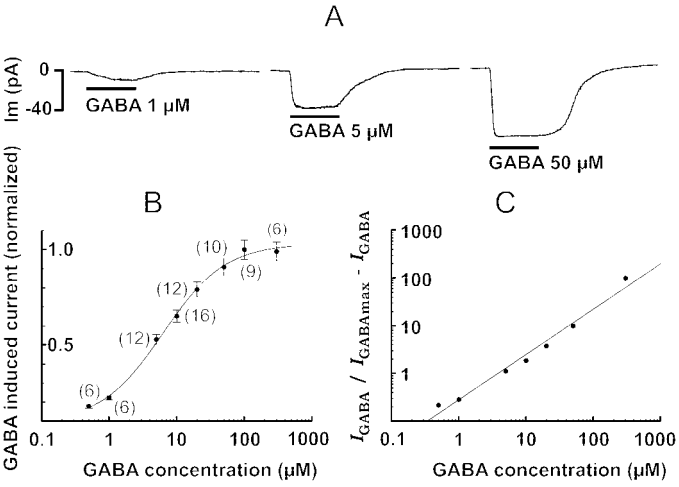

Figure 7. Effects of GABA at the chloride equilibrium potential; isolation of the sodium inward current. *A*, Responses to different GABA concentrations obtained in the whole-cell voltage-clamp mode at −62.6 mV holding potential. *B*, Dose–response curve. Each point corresponds to the mean ± SEM; the numbers of cells explored are in parentheses. The mean values were adjusted at sigmoidal function, the EC_{50} of which was 5 μM. *C*, Hill plots with a coefficient equal to 0.95.

solved, but it was mediated by the activation of cation channels (Swensen et al., 2000). From these works, it is clear that different ionic mechanisms are involved in GABA-induced depolarization, but all of them suggest that the GABA actions are mediated by receptors. In contrast, a depolarizing effect mediated by a Na^+-dependent high-affinity system for the uptake of GABA was described in the crayfish stretch receptor neuron (Kaila et al., 1992). In this paper we demonstrate a direct influence of GABA

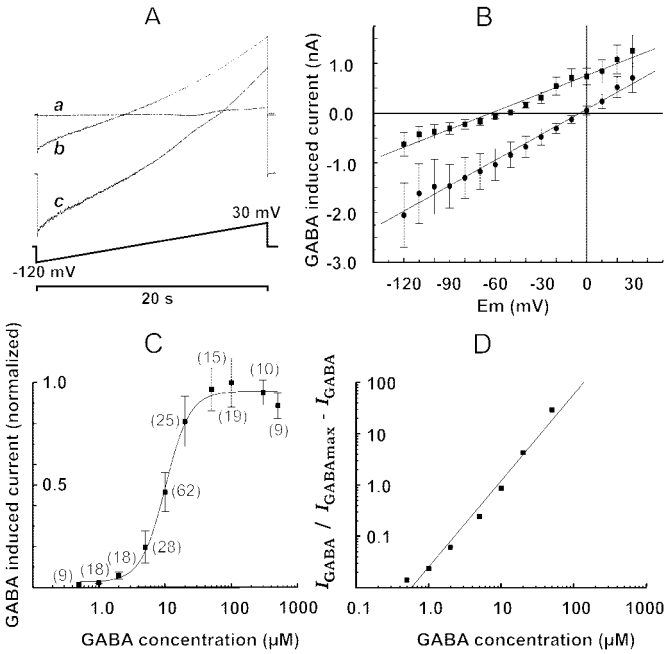

Figure 8. Isolation of the chloride current. *A*, Steady-state currents obtained in the whole-cell voltage-clamp mode after (*a*) and during (*b*, *c*) GABA superfusion in response to voltage ramps from −120 to 30 mV at 7.5 mV/sec. *Traces b* and *c* represent the subtraction between control traces and those obtained during GABA superfusion (100 μM) for E_{Cl^-} of −62.6 and 0 mV, respectively. *B*, Current–voltage relations from 16 (■) and 10 (●) neurons recorded in each experimental condition. The *points* are peak-measured currents. *Lines* were generated by linear regression using a least-squares fit. Note that the experimental reversal potential of the chloride current matches well with the calculated values for the chloride equilibrium potential. *C*, Dose–response relation for the isolated chloride current evoked by GABA concentrations between 0.5 and 500 μM, measured at −60 mV. The mean values were adjusted at sigmoidal function, the EC_{50} of which was 10 μM. Each *point* corresponds to the mean values ± SEM; the numbers of cells explored are in parentheses. *D*, Hill plots with a coefficient equal to 1.7.

uptake on the excitability of the X-organ neurons, which are postsynaptic, because their terminals are specialized for hormonal release and do not establish synaptic contacts with other cells. Our results suggest that circulating GABA levels could be acting tonically on these neurons by operating electrogenic GABA transporters capable of evoking a sustained depolarization associated with neuronal firing.

To provide evidence that the depolarizing effect induced by GABA in the X-organ neurons is mediated by a Na^+-dependent GABA transport system, we reject the proposed possibilities as follows. (1) The response cannot be attributed to bicarbonate (Kaila and Voipio, 1987) because the saline used did not contain bicarbonate, and the cells were recorded with patch pipettes filled with saline buffered with HEPES. (2) The response cannot be attributed to positive chloride equilibrium potential (Hales et al., 1992, 1994) because the isolated chloride response caused by the activation of $GABA_A$ receptors observed in the absence of extracellular Na^+ reversed at the expected values, as we have shown in Figure 8. (3) Finally, the possibility that the depolarizing response could be caused by an increase in cation conductance (Yarowsky and Carpenter, 1978; Swensen et al., 2000) seems improbable because in the absence of extracellular sodium, the potassium driving force operating in the opposite direction would be capable of generating an outward transient current at any membrane potential above its equilibrium potential.

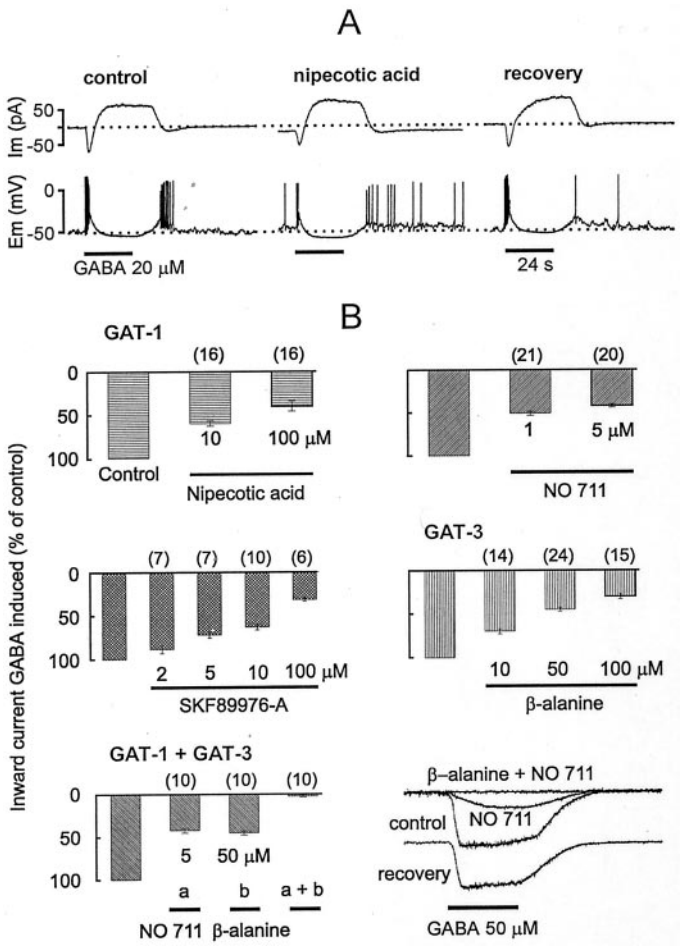

Figure 9. Pharmacology of GABA-induced inward current. *A*, Nipecotic acid blocked partially the sodium current induced by GABA. Current traces were obtained at −50 mV before, during, and after nipecotic acid (10 μM) superfusion. Nipecotic acid evoked a sustained inward current that reduced by ~50% the amplitude of the sodium current induced by GABA and increased the magnitude of the sustained outward current caused by chloride. For comparative proposes, the *bottom traces* obtained from the same cell show changes in membrane voltage. Nipecotic acid induced a sustained depolarization, and during the GABA pulse the early depolarization was brief and followed by a repolarization that reached more negative potentials, suggesting that a minor density of inward current remained active. *B*, Blockage percentage of GABA-evoked sodium current by selective GABA transporter antagonists, GAT-1 (*nipecotic acid*, *NO 711*, and *SKF89976-A*) and GAT-3 (β-alanine). *Horizontal black bars* in the histogram signal the inhibition of the sodium current for each concentration tested, and the numbers of explored cells are indicated in the parentheses. In each experiment the cells were incubated for 5 min in the antagonist, and it was present during GABA superfusion (50 μM). GABA-evoked sodium currents were obtained at the E_{Cl^-} in the whole-cell voltage-clamp mode at −62.6 mV; the washout interval between GABA applications was 5 min. Sequential incubation of NO 711 (5 μM) and β-alanine (50 μM) blocked totally but reversibly the sodium current (*inset traces*).

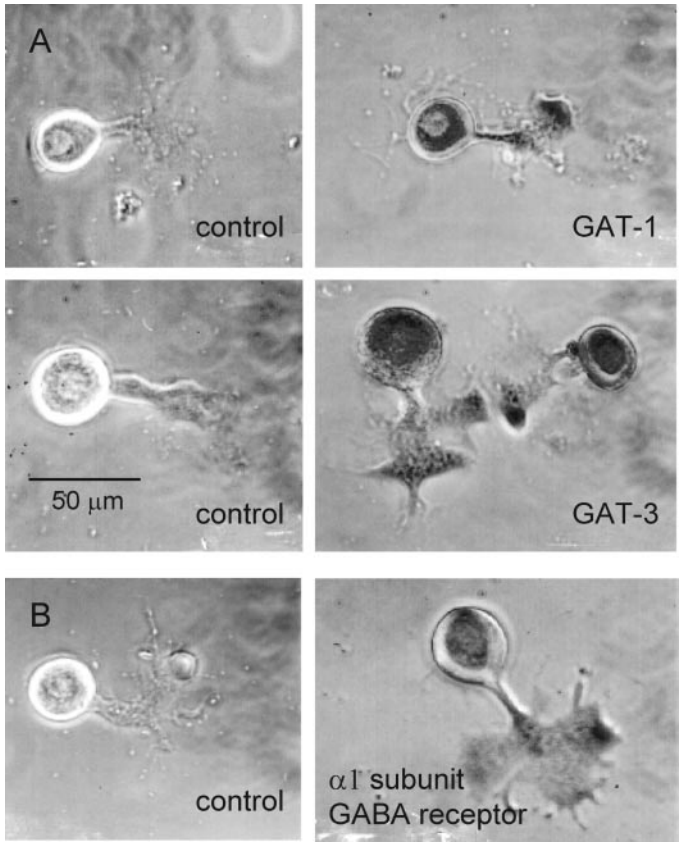

Figure 10. Immunoreactivity for plasma membrane transporters GAT-1, GAT-3, and GABA receptors in X-organ neurons in culture. Control culture cells were nonincubated with the primary antibodies, but they were processed with the avidin–biotin–peroxidase method and revealed with diaminobenzidine. Reactive cells were incubated overnight with the primary antibodies. The entire X-organ cells expressed immunoreactivity for GAT-1 and GAT-3 as well as the α1 subunit of the GABA receptor.

The time course of GABA response in our experimental conditions could be explained by considering the EC_{50} values. We have found an EC_{50} of 5 μM for GABA transporters, whereas $GABA_A$ receptors required higher concentrations (EC_{50} 10 μM) to be activated. The superfusion method that we have used enhanced this behavior, because the neurons were exposed initially to a low GABA concentration and because the transport system is more sensitive; it activated first, and later, when the steady-state concentration was reached, both sodium and chloride currents were present. However, at concentrations between 0.1 and 1.0, μM the sodium current generated by the transporters appears to be predominate (Fig. 2). Most of the radioligand binding studies for $GABA_A$ receptors have characterized two high-affinity binding sites with K_d values in the low and high nanomolar range (Olsen et al., 1981; Olsen and Snowman, 1983). However, most electrophysiological studies have focused on the low-affinity site (micromolar range) (Anthony et al., 1993; Hevers and Lüddens, 1998). Because micromolar concentrations of GABA are generally required for the activation of receptor-gated chloride conductances in electrophysiological experiments (Krespan et al., 1984; Maconochie et al., 1994), it is reasonable to suppose that the lower-affinity agonist binding sites are physiologically relevant (Anthony et al., 1993). The EC_{50} value for the GABA receptor determined here corresponds to the low-affinity binding site. Concentration–response curves for $GABA_A$ receptors are sigmoidal, with Hill coefficients between 1 and 2 (Sakmann et al., 1983; Hattori et al., 1984; Bormann and Clapham, 1985; Pinnock et al., 1988; Sattelle et al., 1991; White, 1992), suggesting that the binding of at least two GABA molecules is required to open the channel. In agreement with these findings, the Hill coefficient for the GABA receptor in X-organ neurons corresponded to 1.7.

The EC_{50} value estimated for GABA transport in X-organ

neurons is comparable to the 5 μM K_m value obtained for GABA uptake both in brain tissue (Martin, 1976; Lewin et al., 1992) and in cells heterologously expressing GAT-1 (Guastella et al., 1990; Keynan et al., 1992; Ye and Sontheimer, 1996). In agreement with previous reports in which the electrogenic uptake of GABA by GAT-1 expressed in *Xenopus* oocytes was explored (Kavanaugh et al., 1992; Mager et al., 1993), our study demonstrates that the Hill coefficient for GABA transporters in X-organ neurons is correlated with voltage-clamp current measurements, suggesting a stoichiometry of one net positive elementary charge per GABA molecule transported.

On the basis of the alternating access model proposed by Hilgemann and Lu (1999), an additional support for the short latency observed in the activation of the inward sodium current is the fact that those ions required for GABA transport are not limiting: they are available because of the superfusion of external solution. The binding of sodium to transporters facilitates GABA binding, and a new conformational state is induced immediately that translocates GABA together with its co-ions. Previous experiments suggest that the ions bond to the transporter despite the absence of GABA, converting the transporter to a state with higher affinity for GABA (Mager et al., 1993, 1996; Cammack et al., 1994). The sodium inward current generated by GABA transport in X-organ neurons was sustained when GABA receptors were blocked (Fig. 7). However, this kinetics depends on the superfusion velocity system used, because faster applications of GABA revealed a biphasic kinetics, as shown previously by Cammack et al., (1994).

In conclusion, GABA evoked on X-organ cells a sodium-dependent inward current sensitive to inhibitors of the GABA transport with an EC_{50} of 5 μM, and simultaneously, but with an EC_{50} of 10 μM, it activates a ligand-gated chloride current sensitive to picrotoxin. The blockage of the sodium-dependent inward current by GABA transport inhibitors supports this notion. In addition, the immunocytochemical evidence suggests that the antibodies against GAT-1, GAT-3, or GABA receptors from vertebrates recognized GABA transporters as well as GABA receptors present in X-organ neurons. Our findings provide experimental support for the hypothesis that hemolymph GABA levels can induce the expression of functional GABA transporters. The expression of GABA transporters is upregulated by extracellular GABA concentration (Bernstein and Quick, 1999). Therefore, the GABA hemolymphatic content in the crayfish could be induced by the expression of GATs in the X-organ sinus gland system. The study of the circadian fluctuations in hemolymph GABA concentration and its relation to the expression of the GATs could be the key to understanding the mechanisms involved in its regulation.

REFERENCES

Alvarado-Alvarez R, Aréchiga H, García U (2000) Serotonin activates a Ca^{2+}-dependent K^+ current in identified peptidergic neurons from the crayfish. J Exp Biol 203:715–723.

Anthony NM, Harrison JG, Sattelle DB (1993) GABA receptor molecules of insects. In: Comparative molecular neurobiology (Pichon Y, ed), pp 172–209. Basel: Birkhäuser Verlag.

Atwood HL (1976) Organization and synaptic physiology of crustacean neuromuscular systems. Prog Neurobiol 7:291–391.

Bernstein EM, Quick MW (1999) Regulation of γ-aminobutyric acid (GABA) transporters by extracellular GABA. J Biol Chem 274: 889–895.

Borden LA, Smith KE, Branchek TA, Weieshank RL (1992) Molecular heterogeneity of the γ-aminobutyric acid (GABA) transport system. J Biol Chem 267:21098–21104.

Bormann J, Clapham DE (1985) γ-Aminoburyric acid receptor channels in adrenal chromaffin cells: a patch-clamp study. Proc Natl Acad Sci USA 82:2168–2172.

Cammack JN, Schwartz EA (1993) Ions required for the electrogenic transport of GABA by horizontal cells of the cat fish retina. J Physiol (Lond) 472:81–102.

Cammack JN, Rakhilin SV, Schwartz EA (1994) A GABA transporter operates asymmetrically and with variable stoichiometry. Neuron 13:949–960.

Clark JA, Deutch AY, Gallipoli PZ, Amara SG (1992) Functional expression and CNS distribution of a β-alanine-sensitive neuronal GABA-transporter. Neuron 9:337–348.

Dingledine R, Boland LM, Chamberlin NL, Kawasaki K, Kleckner NW, Traynelis SF, Verdoorn TA (1988) Amino acid receptors and uptake systems in the mammalian central nervous system. Crit Rev Neurobiol 4:19–30.

Duan S, Cooke IM (2000) Glutamate and GABA activate different receptors and Cl^- conductances in crab peptide-secretory neurons. J Neurophysiol 83:31–37.

Erecinska M (1987) The neurotransmitter amino acid transport systems. Biochem Pharmacol 36:3547–3555.

Gao X, McLean H, Caveney S, Donly C (1999) Molecular cloning and functional characterization of a GABA transporter from the CNS of the cabbage lopper, *Trichoplusia ni*. Insect Biochem Mol Biol 29:609–623.

García U, Aréchiga H (1998) Regulation of crustacean neurosecretory cell activity. Cell Mol Neurobiol 18:81–99.

García U, Grumbacher-Reinert S, Bookman R, Reuter H (1990) Distribution of Na^+ and K^+ currents in soma, axons and growth cones of leech Retzius neurones in culture. J Exp Biol 150:1–17.

García U, Onetti C, Valdiosera R, Aréchiga H (1994) Excitatory action of GABA on crustacean neurosecretory cells. Cell Mol Neurobiol 14:71–88.

Guastella J, Brecha N, Nelson H, Czyzyk L, Keynan S, Miedel MC, Davidson N, Lester HA, Kanner BI (1990) Cloning expression of a rat brain GABA transporter. Science 249:1303–1306.

Hales TG, Kim H, Longoni B, Olsen RW, Tobin AJ (1992) Immortalized hypothalamic GT1–7 neurons express functional γ-aminobutyric acid type A receptors. Mol Pharmacol 42:197–202.

Hales TG, Sanderson MJ, Charles AC (1994) GABA has excitatory actions on GnRH-secreting immortalized hypothalamic (GT1–7) neurons. Neuroendocrinology 59:420–425.

Hattori K, Akaike N, Oomura Y, Kuraoka S (1984) Internal perfusion studies demonstrating GABA-induced chloride responses in frog primary afferent neurons. Am J Physiol 246:259–265.

Hevers W, Lüddens H (1998) The diversity of $GABA_A$ receptors. Pharmacological and electrophysiological properties of $GABA_A$ channel subtypes. Mol Neurobiol 18:35–86.

Hilgemann DW, Lu CC (1999) GAT-1 ($GABA:Na^+:Cl^-$) cotransport function. Database reconstruction with an alternating access model. J Gen Physiol 114:459–475.

Iversen LL, Kelly JS (1975) Uptake and metabolism of γ-aminobutyric acid by neurones and glial cells. Biochem Pharmacol 24:933–938.

Iversen LL, Kravitz EA (1968) The metabolism of γ-aminobutyric acid (GABA) in the lobster nervous system: uptake of GABA in nerve-muscle preparations. J Neurochem 15:609–620.

Kaila K, Voipio J (1987) Postsynaptic fall in intracellular pH induced by GABA-activated bicarbonate conductance. Nature 330:163–165.

Kaila K, Rydquist B, Pasternack M, Voipio J (1992) Inward current caused by sodium-dependent uptake of GABA in the crayfish stretch receptor neurone. J Physiol (Lond) 453:627–645.

Kanner I, Schuldiner S (1987) Mechanism of transport and storage of neurotransmitters. CRC Crit Rev Biochem 22:1–38.

Kavanaugh MP, Arriza JL, North RA, Amara SG (1992) Electrogenic uptake of γ-aminobutyric acid by a cloned transporter expressed in *Xenopus* oocytes. J Biol Chem 267:22007–22009.

Kerkut GA, Pitman RM, Walker RJ (1969) Sensitivity of neurones of the insect central nervous system to iontophoretically applied acetylcholine or GABA. Nature 222:1075–1076.

Keynan S, Suh YJ, Kanner BI, Rudnick G (1992) Expression of a cloned γ-aminobutyric acid transporter in mammalian cells. Biochemistry 31:1974–1979.

Krespan B, Springfield SA, Haas H, Geller HM (1984) Electrophysiological studies on benzodiazepine antagonists. Brain Res 295:265–274.

Krnjevic K (1984) Some functional consequences of GABA uptake by brain cells. Neurosci Lett 47:238–287.

Lewin L, Mattsson MO, Sellstrom A (1992) Inhibition of transporter mediated γ-aminobutyric acid (GABA) release by SKF 89976-A, a GABA uptake inhibitor, studied in a primary neuronal culture from chicken. Neurochem Res 17:577–584.

Liu QR, Lopez-Corcuera B, Mandiyan S, Nelson H, Nelson N (1993) Molecular characterization of four pharmacologically distinct γ-aminobutyric acid transporters in mouse brain. J Biol Chem 268:2106–2112.

Maconochie DJ, Zempel JM, Steinbach JH (1994) How quickly can $GABA_A$ receptors open? Neuron 12:61–71.

Mager S, Naeve J, Quick M, Labarca C, Davidson N, Lester HA (1993)

Steady states, charge movements, and rates for a cloned GABA transporter expressed in *Xenopus* oocytes. Neuron 10:177–188.
Mager S, Kleinberger-Doron N, Keshet GI, Davidson N, Kanner BI, Lester HA (1996) Ion binding and permeation at the GABA transporter GAT1. J Neurosci 16:5405–5414.
Martin DL (1976) Carrier-mediated transport and removal of GABA from synaptic regions. In: GABA in nervous system function (Roberts E, Chase TN, Tower DB, eds), pp 347–386. New York: Raven.
Marty A, Neher E (1995) Tight-seal whole-cell recording. In: Single-channel recording (Sakmann B, Neher E, eds), pp 31–91. New York: Plenum.
Mbungu D, Ross LS, Gill SS (1995) Cloning, functional expression, and pharmacology of a GABA transporter from *Manduca sexta*. Arch Biochem Biophys 318:489–497.
Olsen RW, Snowman AM (1983) [^{3}H]bicuculline methochloride binding to low-affinity γ-aminobutyric acid receptor sites. J Neurochem 41:1653–1663.
Olsen RW, Bergman MO, Van Ness PC, Lummis SC, Watkins AE, Napias C, Greenlee DV (1981) γ-Aminobutyric acid receptor binding in mammalian brain. Heterogeneity of binding sites. Mol Pharmacol 19:217–227.
Pfeiffer-Linn C, Glantz RM (1989) Acetylcholine and GABA mediate opposing actions on neuronal chloride channels in crayfish. Science 245:1249–1251.
Pinnock RD, David JA, Sattelle DB (1988) Ionic events following GABA receptor activation in an identified insect motor neuron. Proc R Soc Lond B Biol Sci 232:457–470.
Quick MW, Corey JL, Davidson N, Lester HA (1997) Second messengers, trafficking-related proteins, and amino acid residues that contribute to functional regulation of the rat brain GABA transporter GAT1. J Neurosci 17:2967–2979.
Sakmann B, Hamill OP, Bormann J (1983) Patch-clamp measurements of elementary chloride currents activated by the putative inhibitory spinal neurons. J Neural Transm [Suppl] 18:83–95.
Sattelle DB (1990) GABA receptors of insects. Adv Insect Physiol 22:1–113.
Sattelle DB, Lummis SC, Wong JF, Rauh JJ (1991) Pharmacology of insect GABA receptors. Neurochem Res 16:363–374.
Swan M, Najlerahim A, Watson REB, Bennett JP (1994) Distribution of mRNA for the GABA transporter GAT-1 in the rat brain: evidence that GABA uptake is not limited to presynaptic neurons. J Anat 185:315–323.
Swensen AM, Golowasch J, Christie AE, Coleman MJ, Nusbaum MP, Marder E (2000) GABA and responses to GABA in the stomatogastric ganglion of the crab *Cancer borealis.* J Exp Biol 203:2075–2092.
White G (1992) Heterogeneity in EC50 and nM of $GABA_A$ receptor currents. NeuroReport 6:461–464.
Yarowsky PJ, Carpenter DO (1978) Receptor for γ-aminobutyric acid (GABA) on *Aplysia* neurons. Brain Res 144:75–94.
Ye Z-C, Sontheimer H (1996) Cytokine modulation of glial glutamate uptake: a possible involvement of nitric oxide. NeuroReport 7:2181–2185.
Yue X, Poosch MS, Whitty CJ, Kapatos G, Bannon MJ (1993) GABA transporter mRNA: in vitro expression and quantitation in neonatal rat and postmortem human brain. Neurochem Int 22:263–270.